Supporting information for

Design of high-performance infrared birefringent crystal $Ba_4HgP_2Se_{10}$ via a low-dimensional motif intercalation strategy

Zhihui Xiong,[a] Haotian Tian,*[b] Zhixi Li,[a] Guowei Deng,*[a] Fang Ding,[a] Qian Wu,[b] and Mingjun Xia*[b]

[a] School of Innovation and Entrepreneurship, Chengdu Normal University, Chengdu 611130, China.

[b] Beijing Center for Crystal Research and Development, Key Laboratory of Functional Crystals and Laser Technology, Technical Institute of Physics and Chemistry, Chinese Academy of Sciences, Beijing 100190, China.

Email: tianhaotian@mail.ipc.ac.cn (H. Tian); guoweideng86@163.com (G. Deng); xiamingjun@mail.ipc.ac.cn (M. Xia)

Table of Contents

Table S1. Crystal Data and Structure Refinement of $Ba_4HgP_2Se_{10}$.

Formula	$Ba_4HgP_2Se_{10}$
Formula weight(g/mol)	1601.49
Crystal system	Triclinic
Space group	$P\bar{1}$
a/Å	6.6236(3)
b/Å	6.9578(3)
c/Å	12.0130(5)
α/°	85.307(4)
β/°	75.875(3)
γ/°	69.438(4)
Volume/Å^3	502.68(4)
Z	1
ρ(calcd) g/cm^3	5.290
μ/mm^{-1}	33.564
F (000)	674
Index ranges	$-8 \le h \le 9$, $-9 \le k \le 10$, $-15 \le l \le 15$
Reflections collected	9620
R_{int}	0.0437
GOF on F^2	1.018
R/wR ($I>2\sigma(I)$)	$R_1 = 0.0298$, $wR_2 = 0.0662$
R/wR (all data)	$R_1 = 0.0381$, $wR_2 = 0.0689$

[a] $R_1 = \Sigma||F_o| - |F_c||/\Sigma|F_o|$ and $wR_2 = [\Sigma w(F_o^2 - F_c^2)^2 / \Sigma wF_o^4]^{1/2}$ for $F_o^2 > 2\sigma(F_o^2)$

Table S2. Atomic coordinates ($\times 10^4$), equivalent isotropic displacement parameters ($Å^2 \times 10^3$) and bond valence sum (BVS) values for $Ba_4HgP_2Se_{10}$.

Atom	x	y	z	U(eq)	BVS
Hg(1)	5000	0	5000	28(1)	2.171
Ba(1)	1218(1)	5912(1)	6318(1)	18(1)	1.927
Ba(2)	5974(1)	1948(1)	1134(1)	18(1)	2.037
Se(1)	1252(1)	11118(1)	1213(1)	15(1)	2.115
Se(3)	5880(1)	7107(1)	1784(1)	19(1)	1.775
Se(5)	4048(1)	3185(1)	3916(1)	16(1)	2.184
Se(2)	1417(1)	5953(1)	1195(1)	19(1)	1.936
Se(4)	345(1)	8656(1)	3861(1)	26(1)	1.741
P(1)	2236(2)	8112(2)	2091(1)	13(1)	4.703

Table S3. Anisotropic displacement Parameters ($Å^2 \times 10^3$) for $Ba_4HgP_2Se_{10}$. The Anisotropic displacement factor exponent takes the form: $-2\pi^2 [h^2a^{*2}U_{11}+2hka^*b^*U_{12}+\ldots]$.

Atom	U_{11}	U_{22}	U_{33}	U_{23}	U_{13}	U_{12}
Hg(1)	29(1)	20(1)	31(1)	10(1)	-7(1)	-6(1)
Ba(1)	17(1)	22(1)	14(1)	-1(1)	-3(1)	-6(1)
Ba(2)	17(1)	22(1)	16(1)	-3(1)	0(1)	-9(1)
Se(1)	16(1)	13(1)	17(1)	3(1)	-4(1)	-5(1)
Se(3)	14(1)	18(1)	24(1)	4(1)	-3(1)	-4(1)
Se(5)	16(1)	16(1)	15(1)	2(1)	-3(1)	-5(1)
Se(2)	21(1)	17(1)	20(1)	0(1)	-4(1)	-10(1)
Se(4)	29(1)	22(1)	13(1)	2(1)	4(1)	1(1)
P(1)	13(1)	12(1)	12(1)	2(1)	-1(1)	-4(1)

Table S4. Bond lengths (Å) and bond angles (°) for $Ba_4HgP_2Se_{10}$.

Hg(1)-Se(5)	2.4395(6)	Ba(2)-Ba(2)#5	4.6715(8)
Hg(1)-Se(5)#1	2.4395(6)	Ba(2)-Se(1)#6	3.4030(7)
Ba(1)-Ba(1)#2	4.3391(8)	Ba(2)-Se(1)#7	3.3524(7)
Ba(1)-Ba(2)#2	4.7878(6)	Ba(2)-Se(1)#8	3.3615(7)
Ba(1)-Ba(2)#3	4.5291(6)	Ba(2)-Se(3)	3.7120(7)
Ba(1)-Se(1)#4	3.4648(7)	Ba(2)-Se(3)#7	3.4131(7)
Ba(1)-Se(3)#3	3.4383(8)	Ba(2)-Se(5)	3.3400(7)
Ba(1)-Se(5)#2	3.3984(7)	Ba(2)-Se(2)#6	3.4200(7)
Ba(1)-Se(5)#3	3.3514(7)	Ba(2)-Se(2)	3.3014(8)
Ba(1)-Se(5)	3.3457(7)	Ba(2)-P(1)#6	3.7643(16)
Ba(1)-Se(2)#2	3.4734(7)	Se(1)-P(1)	2.2198(16)
Ba(1)-Se(4)	3.4387(8)	Se(3)-P(1)	2.2081(16)
Ba(1)-Se(4)#2	3.7081(8)	Se(2)-P(1)	2.1978(17)
Ba(1)-Se(4)#4	3.5540(7)	Se(4)-P(1)	2.1759(16)
Se(5)-Hg(1)-Se(5)#1	180	Se(3)-P(1)-Se(1)	105.11(6)
Se(2)-P(1)-Se(1)	107.33(7)	Se(2)-P(1)-Se(3)	107.78(7)
Se(4)-P(1)-Se(1)	105.94(6)	Se(4)-P(1)-Se(3)	117.39(8)
Se(4)-P(1)-Se(2)	112.59(7)		

#1 -x+1,-y,-z+1 #2 -x,-y+1,-z+1 #3 -x+1,-y+1,-z+1 #4 -x,-y+2,-z+1 #5 -x+1,-y,-z #6 -x+1,-y+1,-z

#7 x,y-1,z #8 x+1,y-1,z #9 x,y+1,z #10 x-1,y+1,z

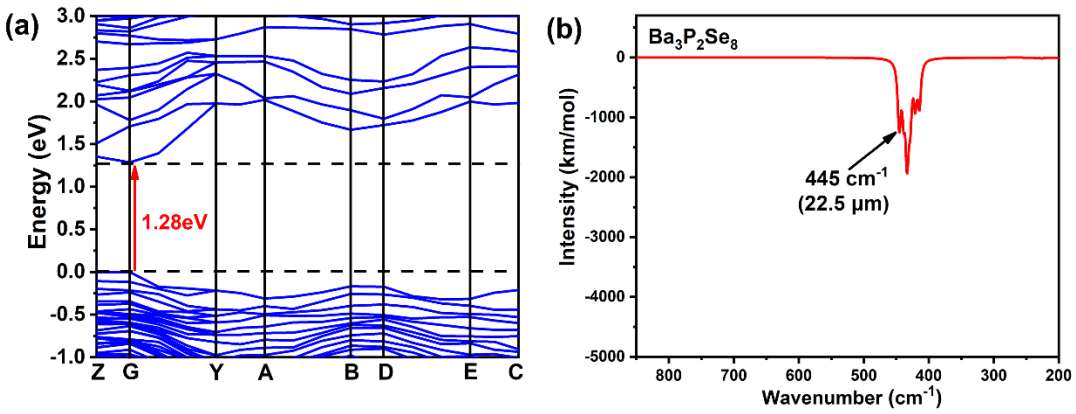

Figure S1. Calculated electronic band structures and infrared spectrum for $Ba_3P_2Se_8$ based on GGA-PBE. (Due to the limitations of the generalized gradient approximation (GGA), PBE methods generally underestimate the bandgap, so this calculated bandgap is in principle lower than the experimental bandgap.)

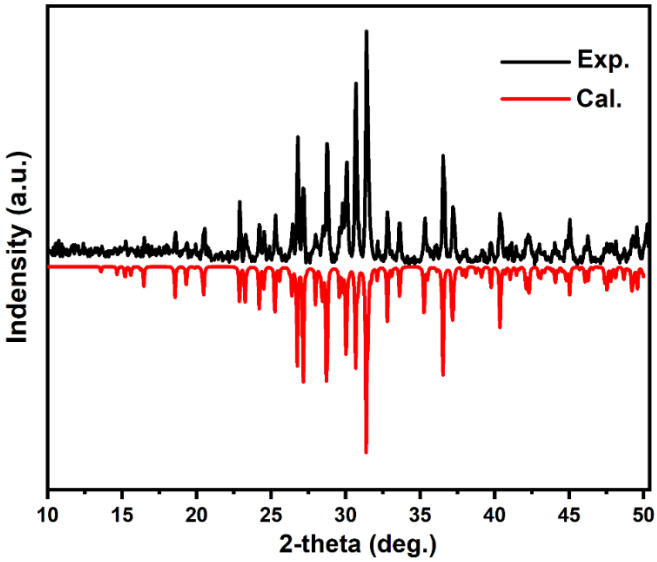

Figure S2. Calculated and experimental powder X-ray diffraction patterns of $Ba_4HgP_2Se_{10}$.

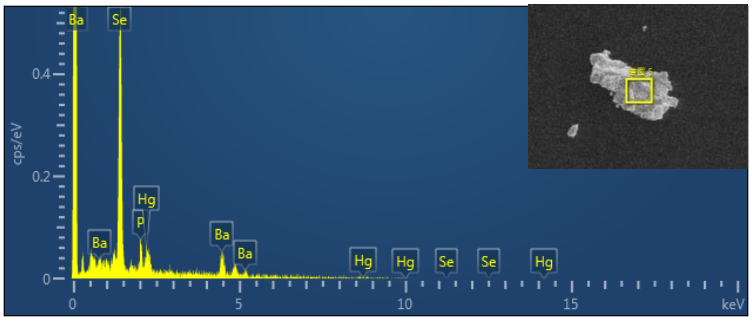

Figure S3. Energy dispersive X-ray spectroscopy analysis of $Ba_4HgP_2Se_{10}$.

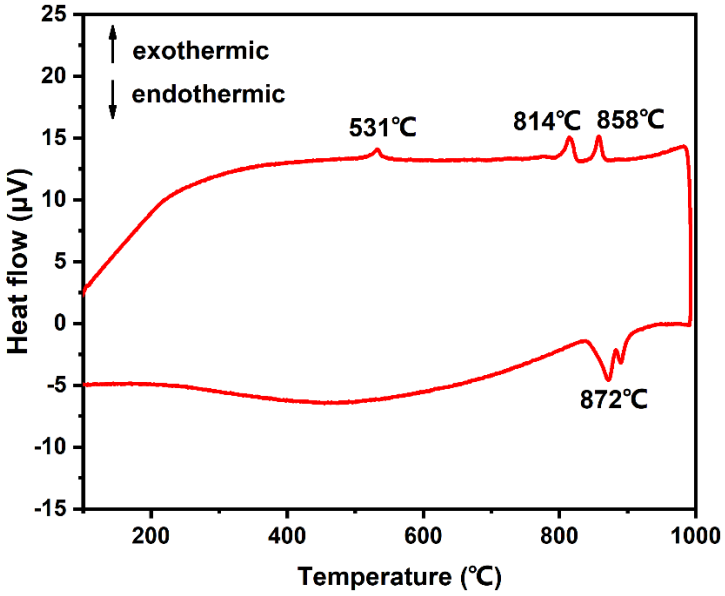

Figure S4. DSC curves of $Ba_4HgP_2Se_{10}$.

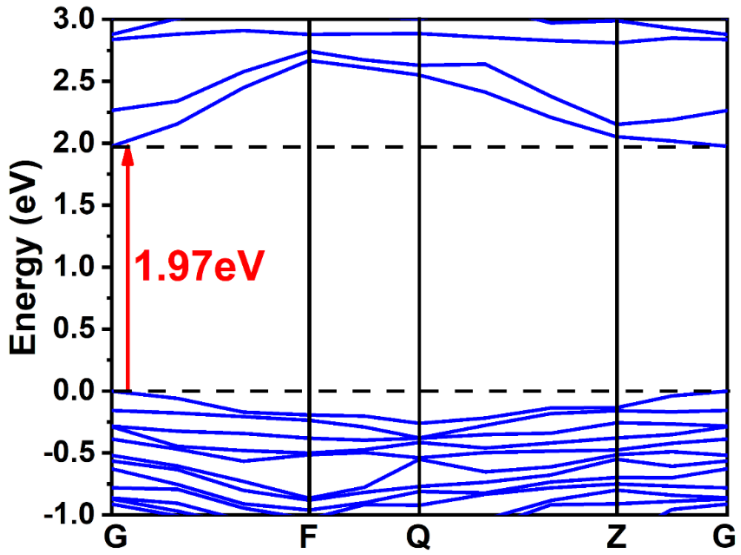

Figure S5. Calculated electronic band structures for $Ba_4HgP_2Se_{10}$ based on GGA-PBE. (Due to the limitations of the generalized gradient approximation (GGA), PBE methods generally underestimate the bandgap, so the value is lower than the experimental value.)

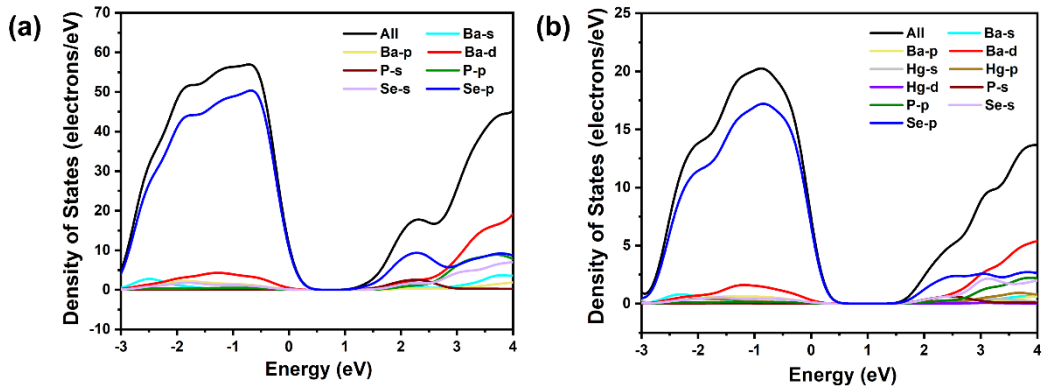

Figure S6. Partial density of states (PDOS) curves for $Ba_3P_2Se_8$ and $Ba_4HgP_2Se_{10}$.

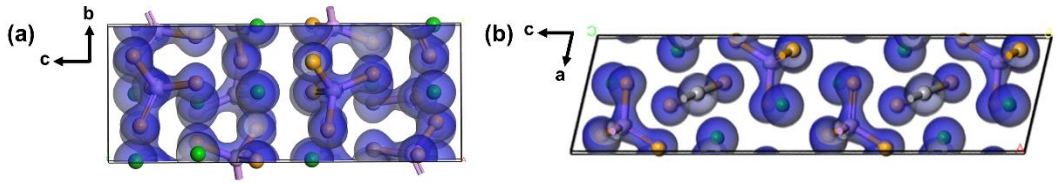

Figure S7. Calculated electron density for $Ba_3P_2Se_8$ and $Ba_4HgP_2Se_{10}$.

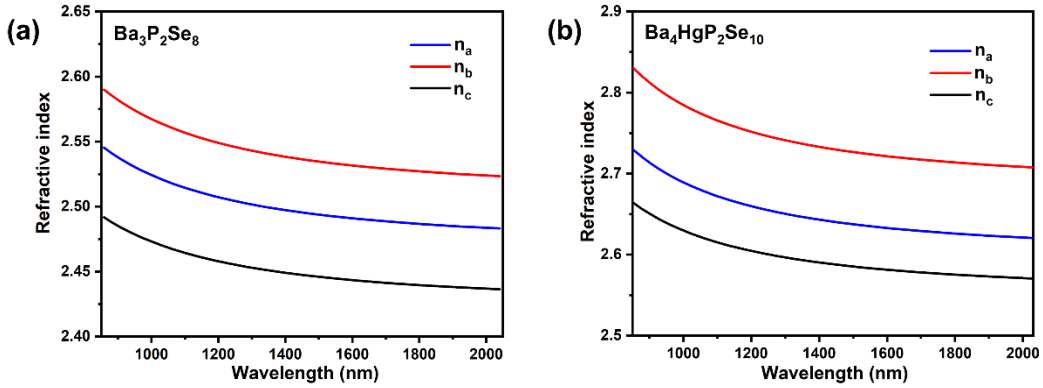

Figure S8. Calculated refractive indices curves for $Ba_3P_2Se_8$ and $Ba_4HgP_2Se_{10}$.